SUPPLIMENTARY INFORMATION

Slippery when wet: mobility regimes of confined drops in electrowetting

Davood Baratian[1], *Élfego Ruiz-Gutiérrez*[2], *Frieder Mugele*[1], *Rodrigo Ledesma-Aguilar*[2]

[1] Physics of Complex Fluids, MESA+ Institute for nanotechnology, Department of Science and Technology, University of Twente, The Netherlands

[2] Smart Materials and Surfaces Laboratory, Faculty of Engineering and Environment, Northumbria University, Ellison Place, Newcastle upon Tyne, NE1 8ST, UK

S1. Reconfiguration of droplet under electrowetting

In the inwards motion of droplet, upon applying the electrical potential, the contact angle decreases abruptly which leads to the movement of the droplet towards the apex of the wedge. The time evolution of the curvature corresponding to the upper and lower interfaces at each and every time instant, are very similar to each other during this translation (see the variation of radii of fits to the upper and lower interfaces). There is a fast increase just after the voltage is applied due to spreading of droplet over the wedge walls, and then the radii decay together to a value corresponding to drop's radius in its new equilibrium configuration. It implies that the pressure inside the droplet is equilibrated quickly, but not the contact angles. Figure S1 shows that the contact angle at the bottom is slightly larger compared to the top one throughout the translation. The contact angle at the top and bottom interface represent the advancing and receding contact angles respectively as the droplet approaches the apex of the wedge. Both the angles decrease upon applying voltage and eventually reach the Young-Lippmann angle

of $\theta_e = 123° \pm 2.32°$ at 100 V rms. However, the lower (advancing) contact angle takes more time to decay to this asymptotic value. The spherical shape of droplet when it equilibrates after the translation has been manifested by fits to the top and bottom interfaces (green and red circles respectively). We see that; indeed, both the fitting circles are overlapping, meaning that the droplet has the same curvature at top and bottom and both the interfaces are parts of a single sphere.

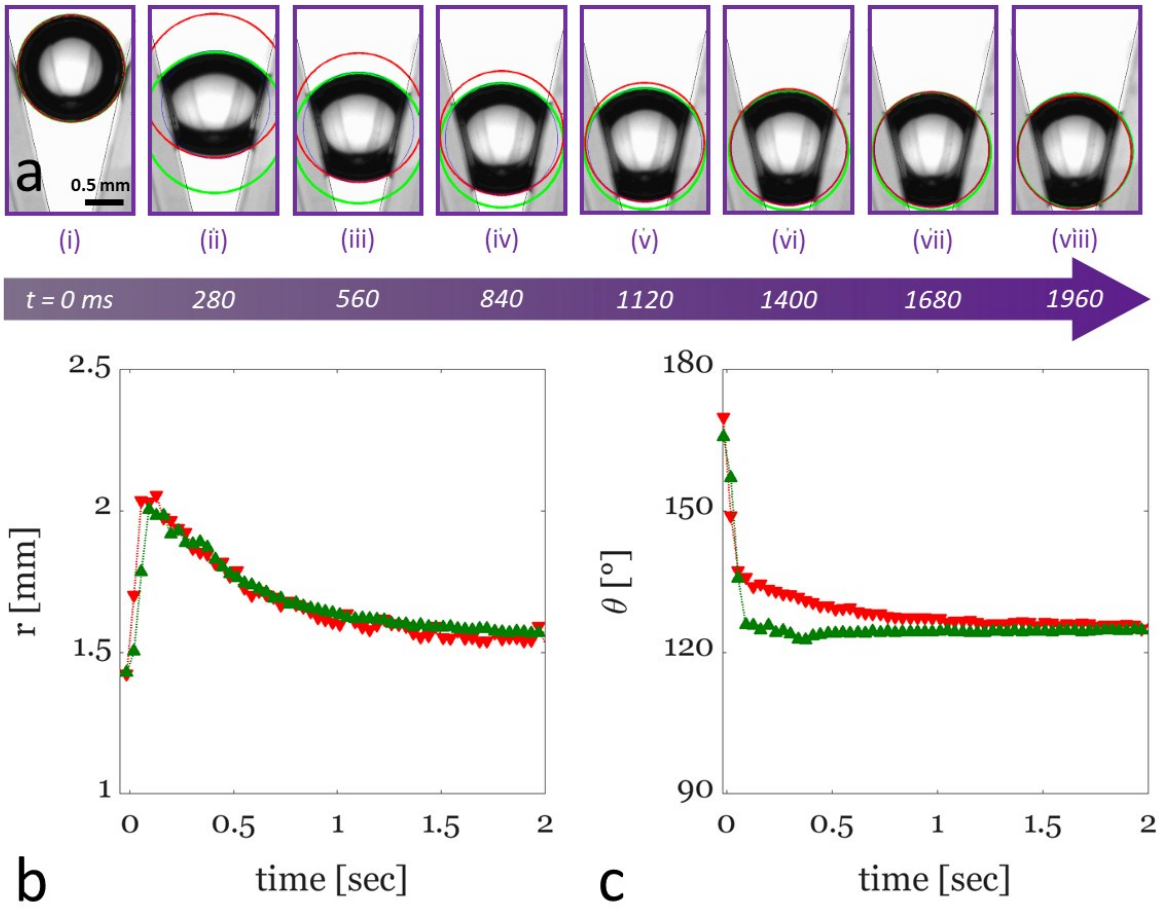

Figure S1: (a) time-lapse images of the drop of V=12 μl in a wedge of opening angle $\beta = 12.5°$ within a time window of ~2 sec starting from EW actuation of U=100 V rms (from left to tight). The series shows drop configuration in the wedge as it translates towards the wedge apex. The red (green) circles shows the fit to the drop's top (bottom) interface at each and every time instants. The time evolution of radii of the fitting circles as well as the top and bottom contact angles are shown in (d) and (e) respectively.

S2. Position of droplet with regards to the wedge apex

In the equilibrium configuration, the position of the droplet is defined as the distance between the center of the sphere from the apex. For out of equilibrium configurations in which the droplet is not a truncated sphere anymore, we consider the intersection of the droplet with the bisector plane of the wedge which is a circle in xz plane. Then we define the position of droplet as the distance of the center of this circle from the apex.

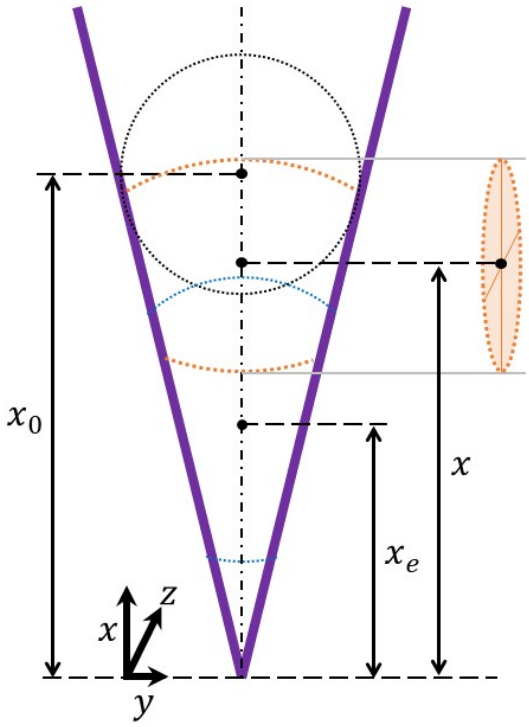

Figure S.2: The position of the droplet is defined as the distance of its center from the wedge apex. The solid lines show the contour of the droplet in initial and final equilibrium configuration while the dashed line represents the out-of-equilibrium profile of the droplet.

S3. Voltage dependent translation of droplet under EW

Figure S3 shows the position of droplet under EW for multiple voltage levels. The droplet is $V = 8\,\mu l$ in volume and the wedge opening angle is $\beta = 9.5°$. While the drop's initial position in inwards motions (terminal position in outwards motion) is the same for all the cases, the terminal (initial) position depends on the applied electrical potential.

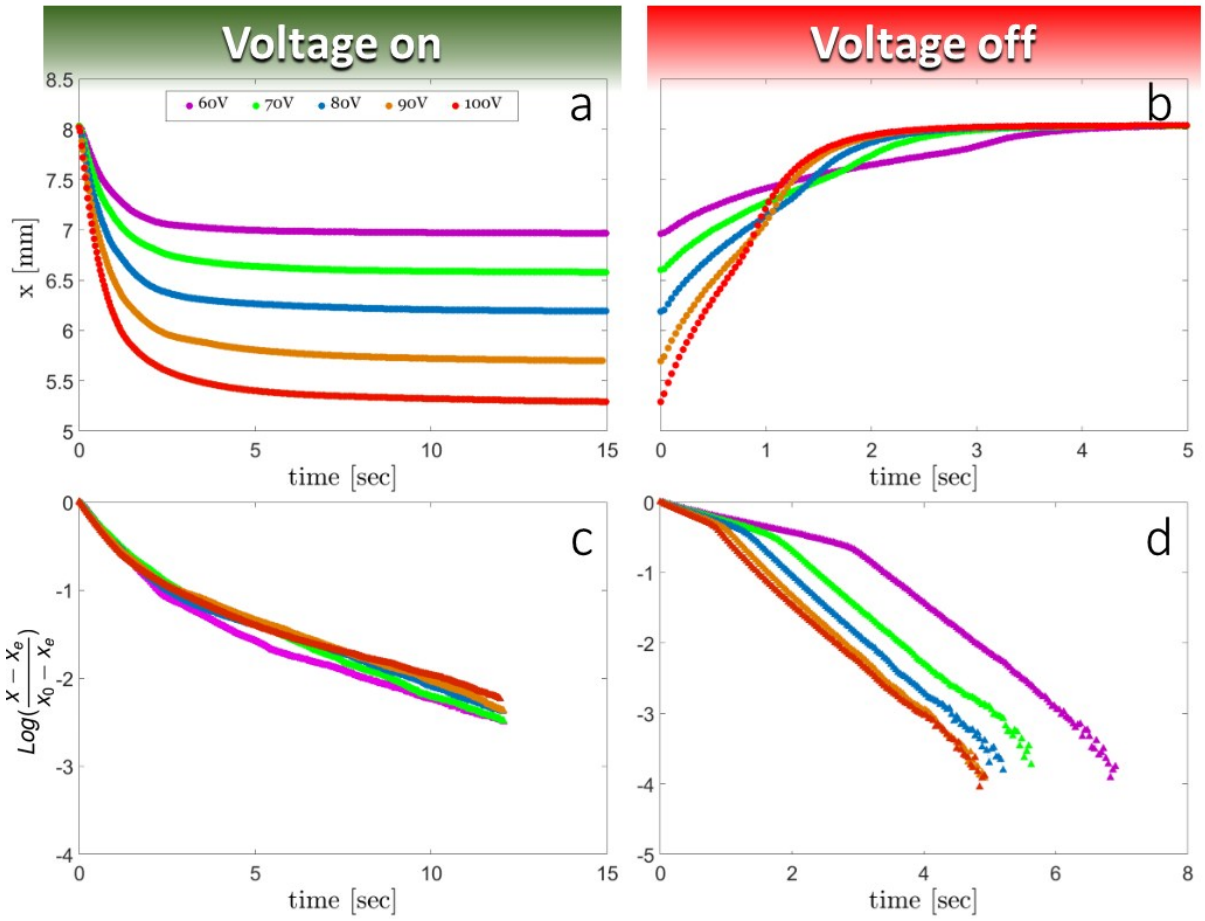

Figure S.3: Translation of a droplet ($V = 8\,\mu l$) in a wedge ($\beta = 9.5°$) under EW at multiple voltage levels from 60,70, 80, 90, and 100 V rms. (a) the inwards translation upon applying the voltage (b) the outwards translation upon removing the voltage. (c) and (d) are the representation of data in logarithmic scale for inwards and outwards translations respectively. The semi-log plots depict more clearly the two relaxation regimes for each case.

S4. The LBM algorithm

The lattice-Boltzmann method integrates the hydrodynamic equations of motion by solving the discretized Boltzmann equation from Kinetic Theory. Our method makes use of three particle distribution functions to solve the hydrodynamic equations coupled with the electrostatics forces. Here, we use the D2Q9 model, i.e., 2-dimensional simulations with a 9-velocity vector set.

The hydrodynamic behavior is modelled by the Navier-Stokes equation, in the incompressible limit,

$$\rho(\partial_t + v \cdot \nabla)v = -\nabla p + \rho\nu\nabla^2 v + f, \qquad (1)$$

where ρ is the density, v is the velocity field, p is the pressure, ν is the kinematic viscosity and f are body forces which include the capillary and electric forces. Eq. (1) is solved by the first lattice-Boltzmann equation

$$f_q(x + c_q, t+1) = f_q(x,t) + \sum_{r=0}^{Q-1} \Lambda_{qr}\left[f - f^{eq}\right]_r(x,t)$$

where x is the discretized position, $\{c_q\}_{q=0}^{Q-1}$ is the set of velocities, and t is the discretized time variable. The momentum density of the fluid mixture is obtained by calculating the first moment of the distribution function, i.e., $\rho v = \sum_{q=0}^{Q-1} c_q f_q$ and the equilibrium distribution function is such that satisfies the relations: $\sum_{q=0}^{Q-1} f_q^{eq} = \rho$, $\sum_{q=0}^{Q-1} c_q f_q^{eq} = \rho v$ and $\sum_{q=0}^{Q-1} c_q c_q f_q^{eq} = \Pi + \rho v v$ where Π is the pressure tensor such that $-\nabla \cdot \Pi = -\nabla p + f$ [1]. We use a multi-relaxation time (MRT) collision operator for stability while setting a large viscosity ratio of the conducting and dielectric phases, ν_c and ν_d, respectively (see [2] for further details).

The boundary conditions are specified following Ref. [3], this is a bounce-back algorithm in which the velocity of the boundaries are prescribed. At the solid walls, the no-slip boundary condition is enforced fixing the velocity $v_{wall}\hat{x}$. The driving velocity of the flow at the openings is prescribed using a parabolic profile of the vertical coordinate y, $v_{open} = \left[v_{wall} - v_0\, y(L_y - y)\right]\hat{x}$, where v_0 is adjusted to keep the fluid-fluid interface at a fixed position at the centre axis of the channel.

To allow motion of the contact lines after the no-slip boundary condition, we include diffusive phenomena by solving the Cahn-Hilliard equation,

$$(\partial_t + v \cdot \nabla)\phi = M\nabla^2\vartheta, \tag{2}$$

where $\phi = \phi(x,t)$ is the phase field, i.e., a quantity that distinguishes the conducting ($\phi > 0$) from the dielectric ($\phi < 0$) phases, M is the mobility set to unity, and ϑ is the chemical potential of the fluid mixture. Eq. (2) is solved by using a second lattice-Boltzmann equation, $g_q(x + c_q, t+1) = g_q^{eq}(x,t)$. We identify the field phase variable with the zeroth moment, $\phi = \sum_{q=0}^{Q-1} g_q$. The corresponding equilibrium distribution function constrained by the identities: $\sum_{q=0}^{Q-1} g_q^{eq} = \phi$, $\sum_{q=0}^{Q-1} c_q g_q^{eq} = \phi v$ and $\sum_{q=0}^{Q-1} c_q c_q g_q^{eq} = M\vartheta I + \phi vv$.

The electrostatic forces are obtained after solving Laplace's equation for the electric potential, ψ, in the dielectric phase

$$\nabla^2\psi = 0, \tag{3}$$

and setting it to the constant $\psi = U$ in the conducting phase.

We used a diffusive process in a similar fashion to relax the electric potential into Eq. (3), this can be done by proposing the third lattice-Boltzmann equation, $h_q(x + c_q, t+1) = h_q^{eq}(x,t)$. The equilibrium distribution function is defined such that,

$\sum_{q=0}^{Q-1} h_q^{eq} = \psi$. The boundary conditions are identical to the evaporation dynamics of Ref. [4], setting a value for the potential at each electrode as an open boundary.

The thermodynamic behavior of the fluids is set by defining the Helmholtz free energy of the fluid mixture, in the diffuse interface approximation,

$$F[\phi,\psi] := \int \left[\frac{3\gamma}{\sqrt{8}l} \left(\frac{\phi^4}{4} - \frac{\phi^2}{2} + \frac{l^2}{2} |\nabla\phi|^2 \right) - \frac{\epsilon}{2} |\nabla\psi|^2 \right] d\Omega + \int \chi\phi dS, \quad (4)$$

where γ is the surface tension, l is a constant related to the interface thickness, and χ is called the wetting potential that can be tuned to change the wettability of the phases, i.e., adjust the contact angle θ_Y, and ϵ is the electric permittivity of the dielectric phase, $d\Omega$ represents a differential element of volume and dS of surface. The chemical potential is given by $\vartheta := \delta F/\delta\phi$, and the electric charge density, $\varrho := -\delta F/\delta\psi$. From these, the capillary and electric forces are expressed as $f := -\phi\nabla\vartheta - \varrho\nabla\psi$. The simulation is contained in a box of size $L_x \times L_y$. All parameters are summarized in Table 1.

Table 1. Simulation parameters.

L_x	400	L_y	60
ν_c	1/12	ν_d	1/3
ρ	1	ϵ	1/3
l	5	γ	8×10^{-3}
d	4	θ_Y	143.62°

References

[1] M. R. Swift, E. Orlandini, W. R. Osborn, and J. M. Yeomans, "Lattice Boltzmann

simulations of liquid-gas and binary fluid systems," *Phys. Rev. E*, vol. 54, no. 5, p. 5041, 1996.

[2] T. Krüger, H. Kusumaatmaja, and A. Kuzmin, "The lattice Boltzmann method: principles and practice." Springer: Berlin, Germany, 2016.

[3] X. Yin and J. Zhang, "An improved bounce-back scheme for complex boundary conditions in lattice Boltzmann method," *J. Comput. Phys.*, vol. 231, no. 11, pp. 4295–4303, 2012.

[4] R. Ledesma-Aguilar, D. Vella, and J. M. Yeomans, "Lattice-Boltzmann simulations of droplet evaporation," *Soft Matter*, vol. 10, no. 41, pp. 8267–8275, 2014.